J. Chem. Sci. Vol. 124, No. 1, January 2012, pp. 141–148.

Vibrational excitation resulting from electron capture in LUMO of F_2 and HCl – A treatment using the time-dependent wave packet approach[#]

BHAVESH K SHANDILYA[a], MANABENDRA SARMA[b,*], SATRAJIT ADHIKARI[c] and MANOJ K MISHRA[a]

[a]Department of Chemistry, Indian Institute of Technology Bombay, Powai, Mumbai 400 076, India
[b]Department of Chemistry, Indian Institute of Technology Guwahati, Guwahati 781 039, India
[c]Department of Physical Chemistry, Indian Association for the Cultivation of Science, Jadavpur, Kolkata 700 032, India
e-mail: msarma@iitg.ernet.in

Abstract. Vibrational excitation cross-sections $\sigma_{v_f \leftarrow v_i}(E)$ in resonant e-F_2 and HCl scattering are calculated from transition matrix elements $T_{v_f \leftarrow v_i}(E)$ obtained using Fourier transform of the cross correlation function $\langle \phi_{v_f}(R) | \Psi_{v_i}(R,t) \rangle$ where $\Psi_{v_i}(R,t) \approx e^{-i\hbar H_{AB^-}(R)t}\phi_{v_i}(R)$. Time evolution under the influence of the resonance anionic Hamiltonian H_{AB}- (AB=F_2/HCl) is effected using Lanczos reduction technique followed by fast Fourier transform and the target (AB) vibrational eigenfunctions $\phi_{v_i}(R)$ and $\phi_{v_f}(R)$ are calculated using Fourier grid Hamiltonian method applied to potential energy (PE) curve of the neutral target. The resulting vibrational excitation cross-sections provide reasonable agreement with experimental and other theoretical results.

Keywords. Vibrational excitation; time-dependent wave packet approach; shape resonance; boomerang model; impulse model.

1. Introduction

The attachment of electron to the atoms and molecules is an important mechanism of electron transmission through gases and thus, it has been a fascinating area to unravel the factors involved in the formation and decay of these anions since decades.[1–35] When an electron collides a diatomic molecule such as AB, a temporary anionic species AB^- is formed. This temporarily formed state is called resonance and can decay by electron emission. The wavefunction of this compound state has a time dependence: $\Psi_n \propto \exp(-iW_n t/\hbar)$ with complex energy: $W_n \equiv E_n - \frac{i}{2}\Gamma_n$.[1] The A and B nuclei move under the effect of this local complex anionic potential W_n.[1] If the shape of the potential barrier of the target determines the trapping of the electron, it is called 'shape resonance',[1] as observed in low energy e-H_2, e-N_2, e-CO scattering, etc. If the AB^- anion has long enough life-time so that at least one vibration is possible, the cross-section profile will show vibrational structure resulting from a distribution of excited vibrational states of the target and the mechanism is said to be '*boomerang type*'.[2,3,5,7,9,14,16,19] As the time evolved ground state wave function of AB gets sufficient time to reflect from the right turning point of E_{AB^-} and to overlap with the final vibrational wave functions of the target molecule, there is a structure in the resonant scattering cross-sections even for the lowest vibrational excitation of the target.[19] An example of *boomerang* mechanism is observed during the formation of $^2\Pi_g N_2^-$ shape resonance in e-N_2 scattering.[2,3,5,7,9,14,16,19] If the life time of AB^- is shorter than its vibrational period, no fine structures are observed in scattering cross-sections and the shape resonance is said to follow the '*impulse model*' as is observed in e-H_2 scattering.[10,11,14,16,17,19]

Electron attachment to F_2 and HCl molecules are two other important prototypical systems of interest and have been studied by many groups both theoretically and experimentally.[20–35] Hall[20] calculated vibrational excitation cross-sections in e-F_2 scattering employing 'Resonant Scattering Theory'[20] and obtained structure less cross-sections for low lying F_2 states. They attributed this to the absence of reflected components in the nuclear wavefunction.

Although only a few groups have studied vibrational excitation cross-sections in e-F_2 scattering, there have been many investigations on dissociative attachment

[#]Dedicated to Prof. N Sathyamurthy on his 60th birthday
[*]For correspondence

studies in electron-F_2 interactions. Hazi *et al.*[22] studied the dissociative attachment (DA) of electron to F_2 by *ab-initio* treatment of electronic and nuclear motion using resonance theory[2,6,8,22] within adiabatic nuclei approximation. In their calculation, 'first order CI (configuration interaction) treatment' was used to obtain ground states of $^1\Sigma_g^+ F_2$ and $^2\Sigma_u^+ F_2^-$. The resultant cross-sections were about two times larger than that of Chantry's experimental data[21] in the 0.15 – 1.5 eV energy range and more significant below 0.15 eV. The reason for this discrepancy might be due to the consideration of the only contribution of resonant $^2\Sigma_u^+ F_2^-$.

Bardsley and Wadhera[23] studied DA in F_2 using resonant scattering theory. They considered a centrifugal barrier which prevents to escape the added electron and supports quasi bound states. The different symmetries of F_2 and F_2^- ground states gave rise to the p-wave barrier,[23] thus preventing auto-detachment. The Morse potential curves of F_2 and F_2^- intersect a little earlier than the equilibrium inter-nuclear separation of F_2. Comparison of these calculated results with the experimentally measured data from Chantry[21] showed good agreement between 0.15 and 1 eV. However, the 0 eV peak that appeared in the experiment could not be explained from their theory.

Berms *et al.*[25] studied dissociative attachment and vibrational excitation of F_2 molecule within the framework of projection operator approach. The cross-sections calculated for dissociative attachment and vibrational excitation were not only dependent on the details of the nonlocal effects but more strongly on the nature of the potential energy curves.

Vibrational excitation in e-HCl scattering has received attention for a long time.[27–35] Rohr and Linder[27] studied vibrational excitation in e-HCl scattering at low energies. They have used crossed beam technique to measure the cross-sections up to 8 eV. The cross-section for the $\upsilon = 1$ level had very sharp peak near to the threshold and broad maxima around 3 eV, followed by a monotonic decrease. The shape was found to be the same throughout the entire range of scattering angles considered for collision. The cross-section in the first peak measured about 1.3×10^{-15} cm^2 and this value confirmed fairly well with that determined by Ziesel.[28] The authors concluded from their results that vibrational excitation in e-HCl scattering was characterized by a resonance involving the $HCl^{-2}\Sigma^+$ state. They referred this type of resonance as virtual state resonance, implying that the potential experienced by the electron is not adequate for binding the electron. However, the dominant s-wave contribution demonstrated the absence of a centrifugal barrier, which was required for shape resonance and thought to be the principal cause of increased vibrational excitation in low energy electron scattering.

Knoth *et al.*[31] and Schafer and Allan[33] observed vibrational excitation of HCl by electron impact near the threshold. Knoth *et al.*[31] reported $\upsilon = 0 \rightarrow 1$ vibrational excitation occurring with rotational transitions and Schafer and Allan[33] measured threshold peaks in the $\upsilon = 0 \rightarrow 1$ and $\upsilon = 0 \rightarrow 2$ excitations. The anisotropy of the angular distribution of electrons near threshold peak shown in the measurement by Knoth *et al.*[31] indicated contribution of waves higher than s waves. Further, Schafer and Allan[21] also displayed the *boomerang* vibrational structure discovered in the experiment of Cvejanovic and Jureta[31] for the $\upsilon = 0 \rightarrow 1$ vibrational excitation.

Theoretical investigations by many groups have been reported on the study of vibrational excitation cross-section in e-HCl scattering.[29,30,32,33,35] Morgan *et al.*[30] applied multi-centre *R*-matrix method along with a non adiabatic treatment of the nuclear motion. They considered two models, where, one of which included the long range polarization potential and the other did not. The results of low energy cross-section for the excitation of $\upsilon = 1$ level showed a sharp threshold peak in one of the models which was absent in the other. Hence, long range polarization effects were responsible for the sharp threshold peak. Fabrikant[29] used *R*-matrix theory to study the vibrational excitation of HCl by slow electrons, where short range interactions were considered. The cross-sections calculated by them were fairly in good agreement with the experimental values in the region of the broad resonance, but very weak near threshold.

It is against this backdrop that we have used the local complex potential (LCP) based time dependent wave packet (TDWP)[36,37] approach to study vibrational excitations in e-F_2 and e-HCl scattering. The objective of the present study is to examine the vibrational excitation cross-sections using the time evolved ground state vibrational wave functions of F_2 and HCl molecules.

2. Method

As discussed elsewhere,[36] in the TDWP approach, the vibrational excitation cross-sections are calculated as

$$\sigma_{v_f \leftarrow v_i}(E) = \frac{8\pi^3}{k_i^2} \left| T_{v_f \leftarrow v_i}(E) \right|^2, \qquad (1)$$

where k_i is the momentum of the incident electron and $T_{v_i \leftarrow v_f}(E)$ is the transition matrix elements.

The transition matrix elements can be calculated from the Fourier transform of the cross-correlation function$\langle\phi_{v_f}(R)|\Psi_{v_i}(R,t)\rangle$[38] and may be expressed as,

$$T_{v_f\leftarrow v_i}(E) = -\frac{i}{\hbar}\int_0^\infty e^{iEt/\hbar}\langle\phi_{v_f}(R)\mid\Psi_{v_i}(R,t)\rangle dt. \tag{2}$$

The $\Psi_{v_i}(R,t)$ represents the time evolution of the vibrational state, $\phi_{v_i}(R)$ of AB (F_2/HCl) molecule effected by the meta stable anionic Hamiltonian H_{AB^-} i.e.,

$$\Psi_{v_i}(R,t) \approx e^{-iH_{AB^-}(R)t/\hbar}\phi_{v_i}(R) \quad \text{with} \tag{3}$$

$$H_{AB^-}(R) = -\frac{\hbar^2}{2\mu_{AB^-}}\nabla^2 + W(R) \quad \text{and} \tag{4}$$

$$W(R) = E_{AB^-}(R) - \frac{i}{2}\Gamma(R). \tag{5}$$

The wave functions $\phi_{v_i}(R)$ and $\phi_{v_f}(R)$ are the target vibrational wave functions of the AB (F_2/HCl)molecule. The Fourier grid Hamiltonian (FGH)[39,40] method has been used to obtain these vibrational wave functions and time evolution of the initial wave function has been done with the help of Lanczos reduction technique followed by fast Fourier transform (LFFT).[41,42] The systematic details about F_2 and HCl molecules are given below for brevity.

2.1 *e-F_2 scattering*

The potential energy curves of F_2 and F_2^- were constructed in the Morse representation[23]

$$V(R) - V(R_e) = D\left[1 - \exp\{\beta(R-R_e)\}^2\right]. \tag{6}$$

The parameters for the neutral state used are: $D^0 = 0.059$, $R_e^0 = 2.66$ and $\beta_0 = 1.61$ (all in atomic units). For anionic state, the parameters: $D^- = 0.047$, $R_e^- = 3.70$ and $\beta_0 = 0.853$ were obtained as best fit values. The width Γ is written as the product of a barrier penetration factor $f(k_v)$ which depends on energy and R, and $\gamma(R)$, a R dependent factor which is independent of energy. Thus,

$$\Gamma = f(k_v)\,\gamma(R), \tag{7}$$

$$f(k_v) = 2\rho^3k^3/\left(1+\rho^2k^2\right), \tag{8}$$

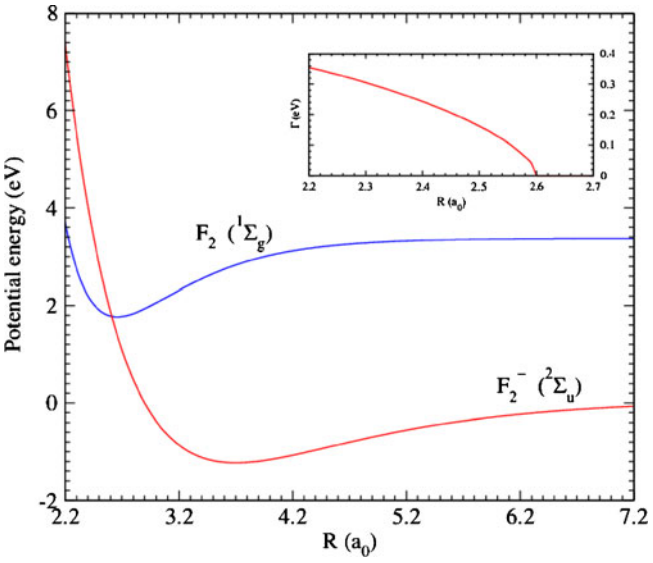

Figure 1. Potential energy curve for F_2 and Re[$W_{F_2^-}(R)$] part of the F_2^- potential $W_{F_2^-}(R)$. Im[$W_{F_2^-}(R)$] part of the $W_{F_2^-}(R)$ potential shown in inset.

$$\gamma(R) = \gamma^0, \quad \text{for } R < R_\gamma, \tag{9}$$

$$\gamma(R) = \gamma^0\exp\left[\alpha\left(R-R_\gamma\right)^2\right], \quad \text{for } R > R_\gamma. \tag{10}$$

Here, k_v is the wavenumber of the emitted electron when the AB molecule is left in the vibrational state v. In the barrier penetration factor, ρ is a measure of a range of short-range interactions and the parameters used in the present calculations are: $\alpha = 1.0$, $R_\gamma = 3.0$, $\gamma^0 = 10.0$.

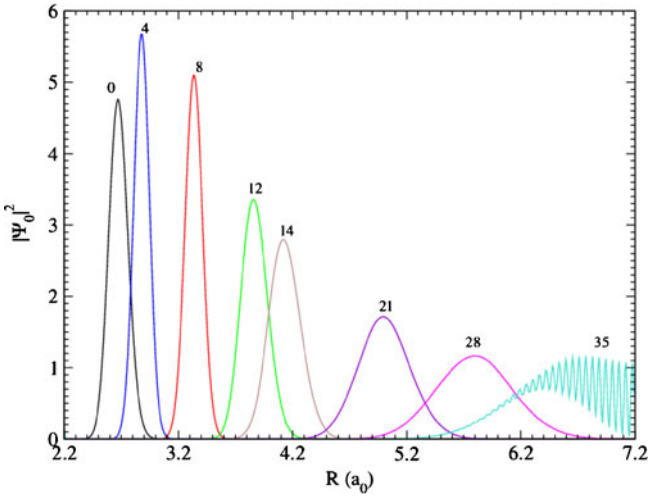

Figure 2. Time evolution of the ground state wavefunction $\phi_0(R)$ of F_2 under the influence of metastable F_2^- Hamiltonian at t = 0, 4, 8, 12, 14, 21, 28 and 35 fs.

2.2 *e-HCl scattering*

The Morse potential of HCl was modified to take into account of the ionic nature of the molecule at larger inter-nuclear distance.[23]

$$V^0(R) = 0.5 - 1/R\left[1 + 1.839\exp\left\{-\beta^0\left(R - R_e^0\right)\right\} - 1.546\exp\left\{-2\beta^0\left(R - R_e^0\right)\right\}\right], \quad (11)$$

where, $\beta^0 = 0.4288$ and $R_e^0 = 2.409$. On the other hand, for the anion

$$E(R) = D^-\exp\left[-2\beta^-\left(R - R_e^-\right)\right] - 2\exp\left[-\beta^-\left(R - R_e^-\right)\right] + A\exp\left(-\alpha R\right). \quad (12)$$

Here, $D^- = 0.0135$, $R_e^- = 3.60$, $\beta^- = 0.70$, $A = 250.0$ and $\alpha = 4.0$. The width function is formulated as that for F_2 with some modification, $f(k_v) = k^{0.33}$, $\gamma^0 = 0.330$ and $R_\gamma = 3.0$. The exponent in $f(k_v)$ considers the long range dipole interaction. The FGH method was employed to generate the cross-correlation functions whose Fourier transform gives the transition matrix elements and the cross-sections [see equation (1)].

3. Results and discussion

3.1 *e-F_2 scattering*

In our calculation, we have used the potential energy curves given by Bardsley and Wadehra[23] for both neutral and anionic species. These potential energy curves of F_2 and F_2^- intersect at an internuclear distance of 2.6 a_0, which is very close to equilibrium separation of (2.66 a_0) of F_2 (figure 1). Time evolution of the ground vibrational state of the neutral F_2 molecule under the

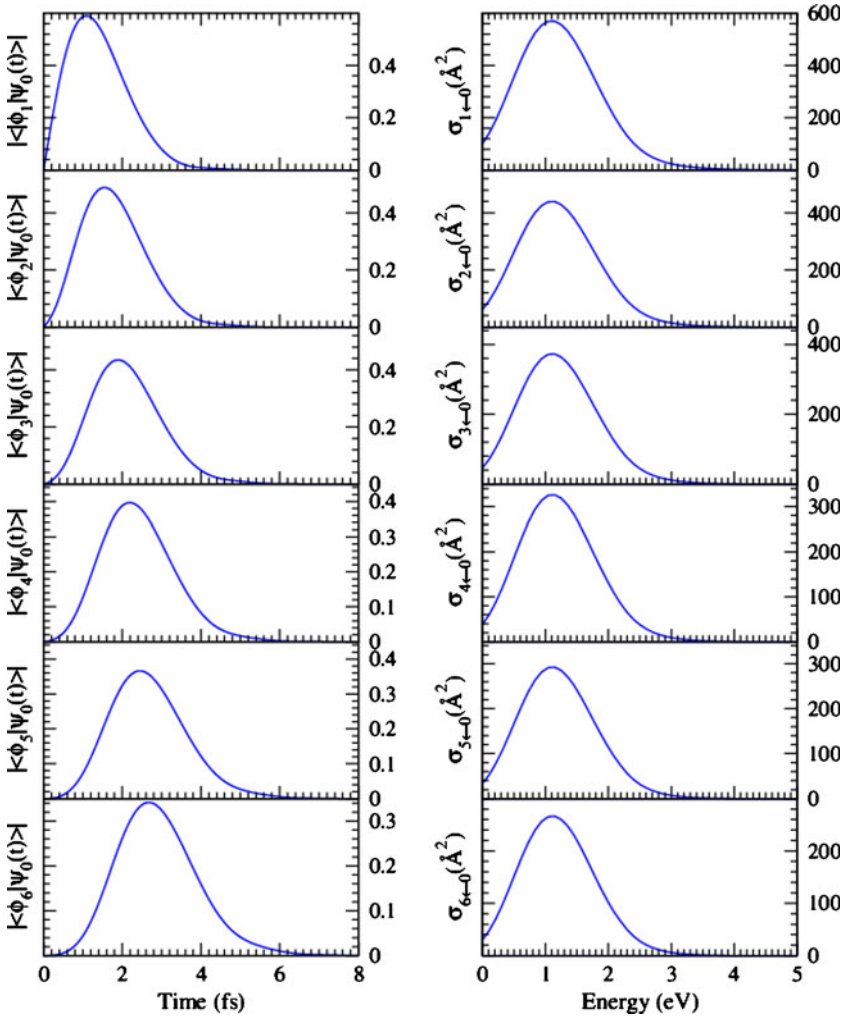

Figure 3. Cross-correlation functions [left six panels] and corresponding vibrational excitation cross-sections [right six panels] for e-F_2 scattering.

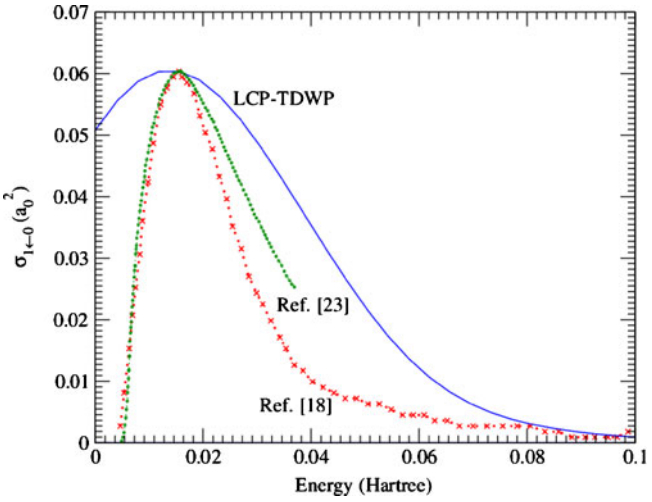

Figure 4. Comparison of vibrational excitation cross-section with other theoretical results of e-F_2 scattering.

influence of the metastable complex F_2^- Hamiltonian is initiated with $\Psi_0(R,t) = \phi_0^{F_2}(R)$ at t = 0 and the wavefunction is propagated with 0.1 a.u. ($\approx$ 0.002 fs) of time step up to nearly 40 fs (no. of time step 16384).

Results from the time evolution of $\Psi_0(R,t) = \phi_0^{F_2}(R)$ at t = 0 under the influence of $^2\Sigma_u^+ F_2^-$ Hamiltonian at t = 4, 8, 12, 14, 21, 28 and 35 fs are presented in figure 2. As we can see in these plots, there is simple diminution of the probability amplitude from 4 fs plot to 35 fs by an order of magnitude. However, between initial probability amplitude plot and 4 fs plot, there is a reversal of values which may be due to the compression of bond from the equilibrium geometry. The peak position of the probability amplitude is moving left to right with time, which implies no reflection from right turning point of the F_2^- curve. One interesting feature of the time evolution plot was the splitting of the wave packet as seen in 35 fs plot in figure 2. The reason for splitting of the wave packet is unknown to us.

The transition matrix elements $T_{1\leftarrow0}$ to $T_{6\leftarrow0}$ were obtained from Fourier transform of the cross correlation functions $\langle\phi_i(R)|\Psi_0(R,t)\rangle$ where $i = 1-6$ as shown in figure 3. The cross correlation functions show only one peak which indicates that there is no reflection of the wave function from the right turning point of the potential energy curve, thereby, justifying *impulse* model for the formation and decay of the $^2\Sigma_u^+ F_2^-$ shape resonance. The vibrational excitation cross-sections $\sigma_{1\leftarrow0}(E)$ to $\sigma_{6\leftarrow0}(E)$ are obtained from the corresponding $T-$ matrix elements, and presented in figure 3. The $\sigma_{1\leftarrow0}(E)$ has been compared with other theoretical calculations[18,23] as shown in figure 4. The relative position of the peak and general profile for energy dependence of $\sigma_{1\leftarrow0}(E)$ agrees quite

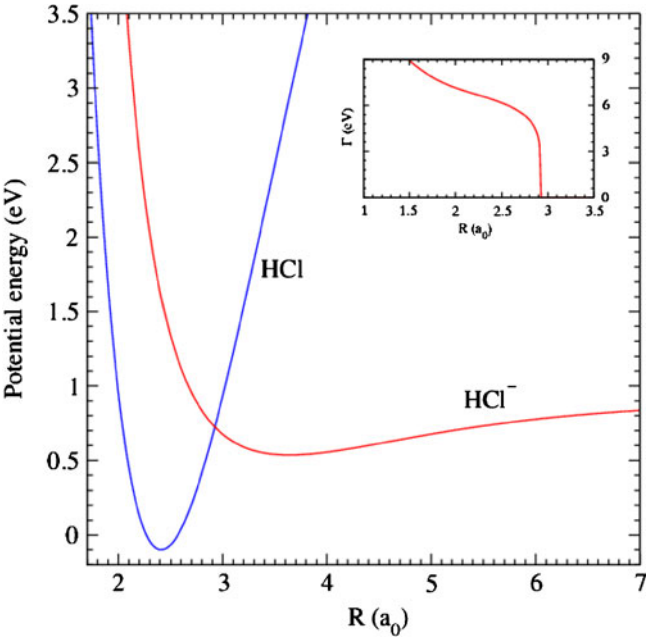

Figure 5. Potential energy curve for HCl and Re[$W_{HCl^-}(R)$] part of the HCl^- potential $W_{HCl^-}(R)$. Im[$W_{HCl^-}(R)$] part of the HCl^- potential $W_{HCl^-}(R)$ shown in inset.

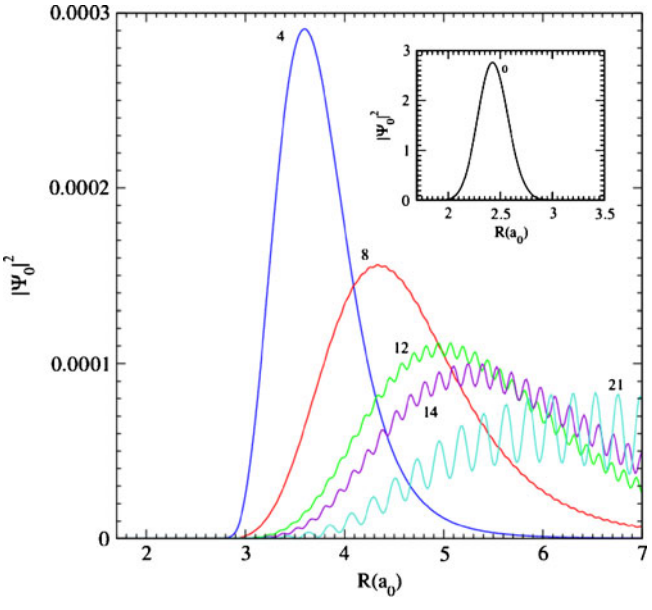

Figure 6. Time evolution of the ground state wave function $\phi_0(R)$ of HCl under the influence of the metastable HCl^- Hamiltonian at t = 4, 8, 12, 14, 21 fs and probability density distribution of the initial wave function of HCl shown in inset.

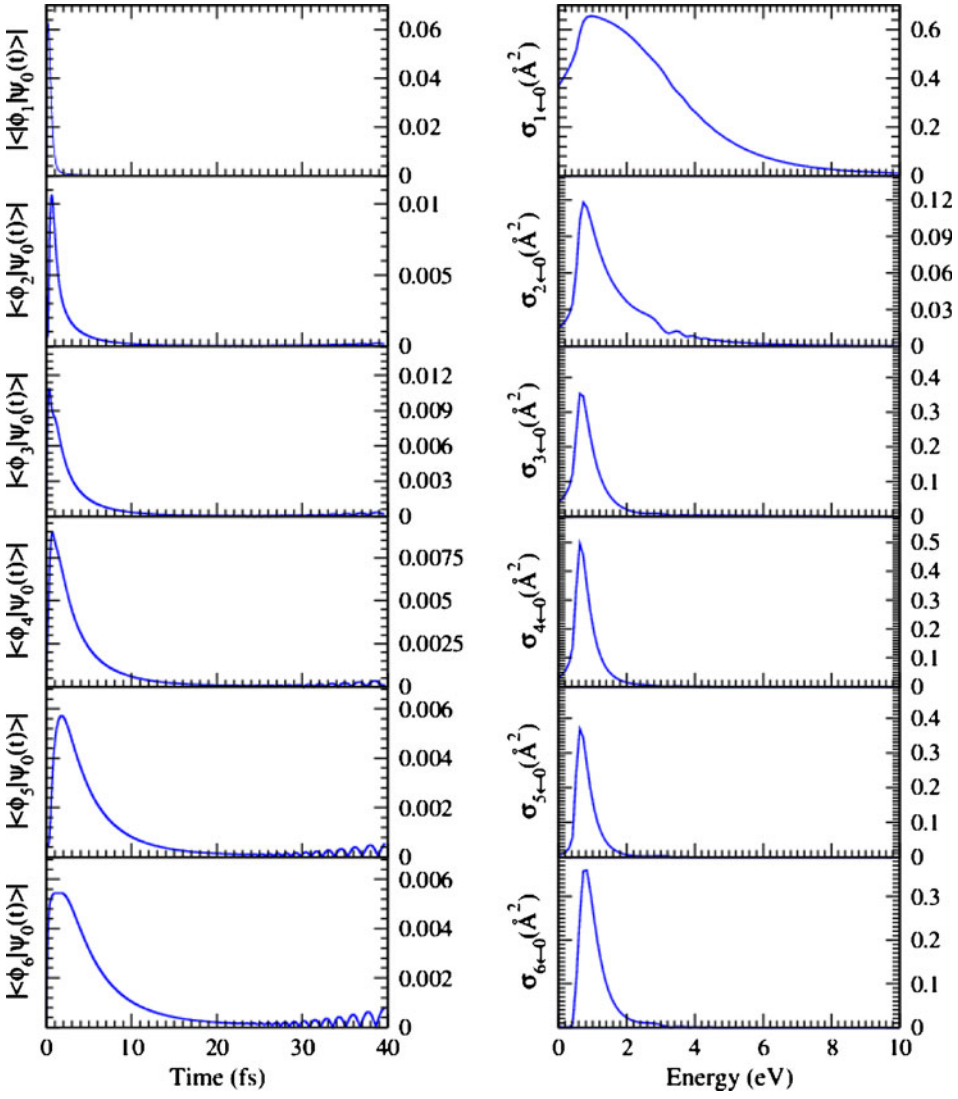

Figure 7. Cross-correlation functions [left six panels] and corresponding vibrational excitation cross-sections [right six panels] for e-HCl scattering.

well with those obtained by other groups.[35] The experimental cross-section for $\sigma_{1\leftarrow 0}(E)$ is not available for comparison.

3.2 *e-HCl scattering*

The potential energy curves of HCl and HCl^- intersect at an internuclear separation of 2.9 a_0 as shown in figure 5. As expected, the width function exponentially decreases to zero at an internuclear separation of 2.9 a_0. Time evolution of the ground vibrational state of the neutral HCl under the influence of the metastable complex HCl^- Hamiltonian begins with $\Psi_0(R,t) = \phi_0^{HCl}(R)$ at t = 0 and such function is propagated in time as that we have used in e-F_2 scattering.

Plot of time evolution of $\Psi_0(R,t) = \phi_0^{HCl}(R)$ at t = 0 under the influence of HCl^- Hamiltonian at t = 4, 8, 12, 14 and 21 fs are presented in figure 6. The diminution of the probability amplitude with time is easily seen in these plots with $|\Psi_0(R,t)|^2$ being 1×10^{-5} at t = 21 fs. The peak position of the probability amplitude is moving from left to right with time, which implies no reflection from right turning point of the HCl^- curve. As we have observed in e-F_2 scattering, the splitting of the wave packet can also be seen here from 12 fs plot itself. The effect is much more prominent than the e-F_2 scattering case.

The transition matrix elements $T_{1\leftarrow 0}$ to $T_{6\leftarrow 0}$ were obtained from Fourier transform of the cross-correlation functions $\langle\phi_i(R)|\Psi_0(R,t)\rangle$ where $i = 1-6$ as shown in figure 7. As in the case of e-F_2

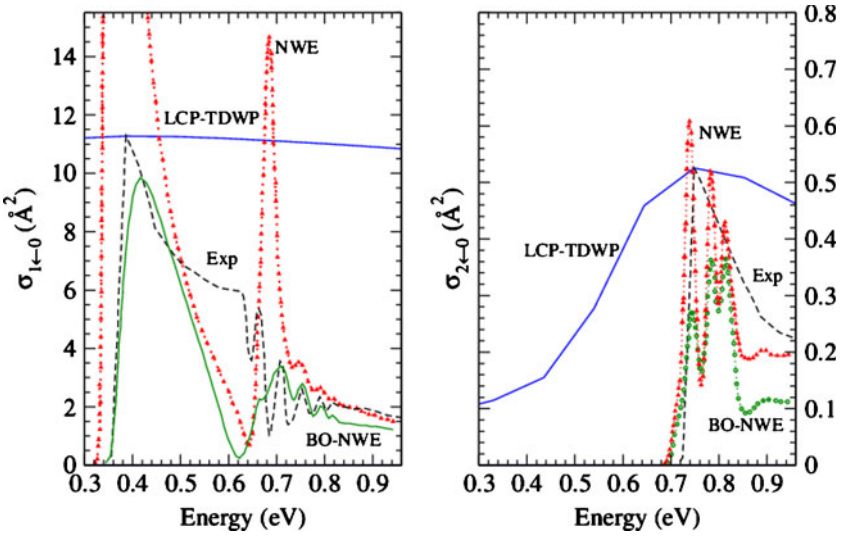

Figure 8. Comparison of vibrational excitation cross-section with other theoretical/experimental results of e-HCl scattering.

scattering, the cross correlation functions do not show any reflection from the right turning point of the potential energy curve, hence classification of e-HCl scattering as *impulse* limit is still valid.

The vibrational excitation cross-sections $\sigma_{1\leftarrow0}(E)$ to $\sigma_{6\leftarrow0}(E)$ obtained from the corresponding $T-$ matrix elements are presented in the right panels of figure 7. The $\sigma_{1\leftarrow0}(E)$ and $\sigma_{2\leftarrow0}(E)$ have been compared with other theoretical calculations and experimental results[34] as displayed in figure 8. The relative position of the peaks and the general profile for energy dependence of $\sigma_{1\leftarrow0}(E)$ and $\sigma_{2\leftarrow0}(E)$ are not in good agreement with experimental and other theoretical results.

4. Concluding remarks

It is our purpose to test our time dependent approach for obtaining vibrational excitation cross-sections as an alternative methodology which is cost effective, and its applicability using local complex potentials to the *impulse* limit of resonance decay. It is seen that a local complex potential based time dependent wave packet approach can determine the vibrational excitation cross-sections of diatomic molecules like F_2, HCl, etc.

The vibrational excitation cross-sections obtained here is highly dependent on nature of potentials which are discussed by Hazi *et al.*[22]. For e-HCl scattering, the cross-section profiles obtained by us are not in good agreement with experimental and other theoretical results. This might be due to the accuracies of potential energy curves and the width function which we have used for nuclear dynamics calculations. For e-F_2 scattering, experimental vibrational excitation cross-section profiles were not reported, so the success of our work cannot be predicted. However, comparison of vibrational excitation cross-sections with other theoretical results show good agreement. The time dependent approach is a unique one because calculations need not to be performed for every incident energy. A time-energy Fourier transform automatically generates the results of entire energy domain. Hence, this is a convenient approach to determine vibrational excitation cross-sections, at least, for diatomics.

Acknowledgements

This research was supported through grants from the Board of Research in Nuclear Sciences (Grant No. 2007/37/41-BRNS/2103) and Department of Science and Technology (DST) (Grant No. SR/S1/PC-30/2006), India to MKM. BKS acknowledges the support from the Council of Scientific and Industrial Research (CSIR), India (SRF, F. No. 09/87(0485)/2007-EMR-I) in the form of a fellowship. MS acknowledges support from IIT Guwahati (Grant No. SG/CHM/P/MS/1). SA acknowledges the Department of Science and Technology (DST), India for partial financial support through the project No. SR/S1/PC-13/2008.

References

1. Bardsley J N and Mandl F 1968 *Rep. Prog. Phys.* **31** 471
2. Birtwistle D T and Herzenberg A 1971 *J. Phys.* **B4** 53

3. Bardsley J N and Biondi M A 1971 *Adv. At. Mol. Phys.* **6** 1
4. Schulz G J 1973 *Rev. Mod. Phys.* **45** 378
5. Schulz G J 1973 *Rev. Mod. Phys.* **45** 423
6. Dube L and Herzenberg A 1975 *Phys. Rev.* **A11** 1314
7. Massey H S W 1976 *Negative ions*, 3rd ed. (Cambridge: Cambridge University Press)
8. Zubek M and Szmytkowski C 1977 *J. Phys.* **B10** L27
9. Dube L and Herzenberg A 1979 *Phys. Rev.* **A20** 194
10. Bardsley J N and Wadhera J M 1979 *Phys. Rev.* **A20** 1398
11. Cederbaum L S and Domcke W 1981 *J. Phys.* **B14** 4665
12. Gauyacq J –P 1987 *Dynamics of negative ions* (Singapore: World Scientific)
13. Domcke W 1991 *Phys. Rep.* **208** 97
14. Sarma M, Adhikari S and Mishra M K 2007 *J. Chem. Phys.* **126** 044309
15. Singh R K, Sarma M, Jain A, Adhikari S and Mishra M K 2007 *J. Chem. Sci.* **119** 385
16. Singh R K, Sarma M and Mishra M K 2007 *Indian J. Phys.* **81** 983
17. Sarma M, Adhikari S and Mishra M K 2008 *Int. J. Quantum Chem.* **108** 1044
18. Houfek K, Rescigno T N and McCurdy C W 2008 *Phys. Rev.* **A63** 012710
19. Sarma M and Mishra M K 2012 *Adv. Quantum Chem.* (in press)
20. Hall R J 1978 *J. Chem. Phys.* **68** 1803
21. Chantry P J 1979 *Bull. Am. Phys. Soc.* **24** 134
22. Hazi A U, Orel A E and Rescigno T N 1981 *Phys. Rev. Lett.* **46** 918
23. Bardsley J N and Wadhera J M 1983 *J. Chem. Phys.* **78** 7227
24. Becker K, McCurdy C, Orlando T and Rescigno T (eds.) 2000 *Current status and future perspective of electron interactions with molecules, clusters, surfaces and interfaces* (Hoboken NJ: Stevens Institute of Technology)
25. Brems V, Beyer T, Nestmann B, Meyer H and Cederbaum L S 2002 *J. Chem. Phys.* **117** 10635
26. Horacek J. and Tarana M 2007 *J. Chem. Phys.* **127** 154319
27. Rohr K and Linder F 1975 *J. Phys.* **B8** L200
28. Ziesel J P, Nenner I and Schulz G J 1975 *J. Chem. Phys.* **63** 1943
29. Fabrikant I I 1985 *J. Phys.* **B18** 1873
30. Morgan L A and Burke P G 1988 *J. Phys.* **B21** 2091
31. Knoth G, Radle M, Gote M, Erhardt H, and Jung K 1989 *J. Phys.* **B22** 299 and references there in
32. Morgan L A, Burke P G and Gillan C J 1990 *J. Phys.* **B23** 99
33. Schafer O and Allan M 1991 *J. Phys.* **B24** 3069
34. Vanroose W, McCurdy C W and Rescigno T N 2003 *Phys. Rev.* **A68** 052713
35. Fedor J, Winstead C, McKoy V, Cizek M, Houfek K, Kolorenc and Horacek, J 2010 *Phys. Rev.* **A81** 042702
36. McCurdy C W and Turner J L 1983 *J. Chem. Phys.* **78** 6773
37. Schneider B I, Dourneuf M L and Lan V K 1979 *Phys. Rev. Lett.* **12** 1365
38. Heller E J 1981 *Acc. Chem. Res.* **14** 368
39. Marston C C and Balint-Kurti G G 1989 *J. Chem. Phys.* **91** 3571
40. Balint-Kurti G G, Dixon R N and Marston C C 1992 *Int. Rev. Phys. Chem.* **11** 317
41. Leforestier C, Bisseling R H, Cerjan C, Feit M D, Friesner R, Guldberg A, Hammerich A, Jolicard G, Karrlein W, Meyer H D, Lipkin N, Roncero O and Kosloff R 1991 *J. Comput. Phys.* **94** 59
42. Kosloff D and Kosloff R 1983 *J. Comput. Phys.* **52** 35